Jundishapur J Health Sci. 2020 October; 12(4):e107662. doi: 10.5812/jjhs.107662.

Published online 2020 December 29. **Research Article**

Cheap Nano-Adsorbents Based on Zno/Mineral Nanocomposites for Removal of Chloroform from Water Solution

Farzad Salehi-Babarsad [1], Ehsan Derikvand [1,*], Majid Razaz [1], Ramin Yousefi [2] and Abbas Shirmardi [3]

[1] Department of Civil Engineering-Water Resources Engineering and Management, Shoushtar Branch, Islamic Azad University (I.A.U), Shoushtar, Iran
[2] Department of Physics, Masjed-Soleiman Branch, Islamic Azad University (I.A.U), Masjed-Soleiman, Iran
[3] Department of Chemistry, Masjed-Soleiman Branch, Islamic Azad University (I.A.U), Masjed-Soleiman, Iran

[*] *Corresponding author*: Department of Civil Engineering-Water Resources Engineering and Management, Shoushtar Branch, Islamic Azad University (I.A.U), Shoushtar, Iran. Email: ederikvand10@gmail.com

Received 2020 July 19; **Revised** 2020 November 16; **Accepted** 2020 November 18.

Abstract

Background: Chloroform, as a hazardous chemical, can contaminate water resources via the reaction of chlorine as an antiseptic chemical with humic acids resulted from agricultural activities. In humans, chloroform may cause dizziness, heart disorders, and disorders of the nervous system. Hence, its removal is of crucial importance.
Objectives: The current study aimed to propose cheap and efficient adsorbents to remove chloroform from water.
Methods: Four different nanomaterials (ZnO, ZnO/graphene oxide (ZnO/GO), ZnO/GO/Zeolite, and GO/Zeolite nanocomposites) were prepared and characterized with X-ray diffraction (XRD), field emission scanning electron microscopy (FESEM) images. Textural properties of the nano- adsorbents were evaluated using Brunauer Emmet Teller (BET) and Barrett-Joyner-Halenda (BJH) techniques. Different isotherms and kinetic models were studied. The effect of pH on the removal efficiency of the nano-adsorbents was tested. Regenerability of the nano-adsorbents towards the removal of the chloroform was also evaluated.
Results: XRD patterns and FESEM images of the nanocomposites confirmed lattice structures and nanoscale particle size of the prepared nanocomposites. According to the BET and BJH models, all samples had mesoporous structures. The BJH cumulative surface area of pores of ZnO, ZnO/GO, ZnO/GO/Zeolite, and GO/Zeolite nanocomposites were 8.5, 26.4, 17.2, and 20.8 m^2/g, respectively. The best removal speed and efficiency were obtained according to the different isotherm and kinetic models for the removal of chloroform ZnO/GO nanocomposites. All adsorbents revealed characteristic adsorption in the pH range of 7 to 8.
Conclusion: The ZnO/GO, a cheap and efficient nanocomposite, showed the best performance to remove chloroform from water samples due to its superior textural property. Hence, it can be used to remove chloroform from water for up to 5 cycles.

Keywords: ZnO nanoparticles, Graphene oxide, Chloroform, Adsorption, BET

1. Background

Water treatment is a major challenge in water engineering science because of extensive contamination of surface and underground waters with chemicals (1). Halogenated hydrocarbons are widely used to synthesis pesticides and herbicides as well as for preparing detergents. Over time, they have contaminated water resources, which resulted in the production of halogenated hydrocarbons (2). Besides, the propagation of such chemicals in the water resources causes their emission into the soil and atmosphere. Hence, such contaminations are not only a great public health challenge but also can deplete the ozone layer (3). In humans, these compounds cause dizziness, heart disorder, and disorders of the nervous system (4-6). Trichloromethane (chloroform) is one of the most abundant halogenated hydrocarbons found in water resources because of the extensive use of chlorine as an antiseptic compound that can produce chloroform through reacting with humic acids (7).

One of the well-known catalysts for chloroform removal is Pt/Pd NPs., which are not cost-effective for commercial applications (8). Hydro-dechlorination is another approach to degrade chloroform; however, this method requires a high-temperature treatment (9-16), indicating that this method is not a cost-effective alternative. Moreover, this method has the drawback of producing toxic byproducts such as phosgene and furan (17, 18). Adsorption of pollutants is a favorable technique to remove hydrocarbons due to its simplicity, non-destructiveness, and being cost-effective (12, 16, 19-23). By using electromagnetic induction, the Fenton like process was applied for the removal of chloroform. Other adsorbents, such as snow, bran rice, and

mud, were also applied for the remediation of chloroform from water resources (12, 16, 23-25).

Nano-adsorbents are good candidates for the adsorption of chemical species because of their large specific surface area, pore-volume, and maximum adsorption capacity (10, 26-29). Zinc oxide NPs are reported as good nano-adsorbents in this regard; hence, several studies have used these compounds as good photocatalytic material and adsorbent, but due to agglomeration of ZnO NPs, it is necessary to use substrates, such as GO, zeolites, and the other organic polymers (30-39). Meanwhile, the application of inorganic substrates is favored because of less toxicity and ease of preparation compared to the organic substrates (9). In this work, two different inorganic substrates (zeolites and GO sheets) were impregnated with zinc oxide NPs to overcome the agglomeration problem of ZnO NPs and hence to enhance its textural properties to achieve a better chloroform removal efficiency.

2. Objectives

The current study aimed to propose cheap and efficient adsorbents to remove chloroform from water.

3. Methods

3.1. Materials

Zinc sulfate, sodium hydroxide, and hydrochloric acid were obtained from Merck, Germany. HPLC grade chloroform from Fluka (Switzerland) was used without further purification. Natural zeolite NPs were purchased from Tamad-Micro Inc. Ultrapure water (Millipore) was used through the work.

To prepare chloroform samples, a 500 mg. L^{-1} chloroform stock solution was prepared by dissolving the appropriate volume of pure chloroform into 1L of ultrapure water in a volumetric flask. It was then used to prepare other diluter chloroform samples.

3.2. Synthesis

ZnO NPs were prepared as described in our previous work (9). The prepared ZnO NPs were used as a support for preparing the nanocomposites. ZnO/GO was prepared as described earlier (9, 38). For preparing ZnO/GO/Zeolite or GO/Zeolite nanocomposites, at first, the purchased zeolites were washed with plenty of ultra-pure water to remove ionic salts within the zeolite pores. So that 0.5 g of the zeolite weighted in a beaker, 0.5 g of ZnO NPs, and 0.1 g of GO was added to it, then 20 mL of ultrapure water was added to the mixture. The mixture was sonicated for 1 h. Afterward, it was placed over a magnetic stirrer for stirring overnight.

3.3. Experimental Procedure

Five different 100, 75, 50, 25, and 10 mg. L^{-1} chloroform solutions were prepared, and then 20 mL of each of them was poured into four beakers containing 20 mg of the four nano-adsorbents, ZnO, ZnO/GO, GO/zeolite, and ZnO/GO/zeolite. The nano-adsorbents/chloroform mixtures were stirred over stirrers for 30 min. Then the mixtures were filtered. After that, 1 μL of each of the filtrates were presented to the GC to measure the equilibrium concentrations of chloroform and hence to obtain adsorption isotherm models.

50 mL of 50 mg. L^{-1} solution was poured into the different beakers containing 20 mg of the different adsorbents. The mixtures were placed over the stirrer, and 5 mL of the samples were taken after each 10 min duration time. Each of the taken mixtures was centrifuged to remove the adsorbents, and then 1 μL of the clear solutions were presented to GC to measure the remained chloroform concentrations.

To study the effect of pH on the adsorption of chloroform, various 50 $mg.dm^{-3}$ chloroform solutions were prepared in different pHs. A metrohm 780 pH/ion-meter was used to monitor pH. Adjustment of pH was performed by adding appropriate amounts of sodium hydroxide salt and/or hydrochloric acid into the chloroform solutions.

3.4. Analysis

Concentrations of chloroform were measured using a gas chromatograph (GC), Varian CP-3800, Australia, equipped with a 300 mm, 0.32 mm in diameter column #cp 8752, flame ionization detector, 1177 split injector. Helium gas was used as carrier gas. The GC column worked over-temperature ranged from 35°C to 120°C BJH and BET models, based on N_2-adsorption-desorption at 77K, were performed with (BElSORP Mini (Microtrac Bel Corp CO)) to determine the pore diameter, pore volume, and active surface area of the nanocomposites. XRD patterns were obtained with X'Pert Pro (Panalytical Co.). The FESEM images were taken with Sigma VP, Zeiss, Germany.

Kinetic studies of adsorption phenomena are good keys to derive information about the adsorption mechanism. Different adsorption kinetic models, pseudo-first-order, pseudo-second-order, and inter-particle diffusion were introduced by the authors (40-44). Equilibrium adsorption capacity (q_e) and instantaneous adsorption capacity (q_t) were measured according to Equations 1 and 2.

$$q_e = \frac{(C_o - C_e) \times V}{m} \quad (1)$$

$$q_t = \frac{(C_o - C_e) \times V}{m} \quad (2)$$

Where C_0, and C_e are initial and equilibrium concentrations of chloroform, respectively. To fit the pseudo-first-order kinetic model of the adsorbents, the corresponding q_e and q_t were fitted in Equation 3. In the following Log (q_e- q_t) was plotted versus t (40, 41). So that intercept of the straight-line produced log q_e, and its slope presents the rate constant of the pseudo-first-order adsorption rate constant, K_1:

$$log\,(q_e - q_t) = logq_e - \frac{k_1}{2.303}t \quad (3)$$

The pseudo-second-order kinetic model was obtained by regressing $^{t}/_{q_t}$ versus t (Equation 4) (42). So that the pseudo-second order rate constant, K_2, and equilibrium adsorption capacity of the adsorbent were obtained from intercept and slope of the regression line, respectively. Squared correlation coefficient of the regression line gives the goodness of fit to the adsorption kinetic models:

$$^{t}/_{q_t} = \frac{1}{K_2\, q_e^2} + \frac{1}{q_e}\ t \quad (4)$$

Inter-particle diffusion model was obtained by regressing qt versus $t^{1/2}$ (44):

$$q_t = K_p t^{1/2} + x_t \quad (5)$$

Where K_p is the inter-particle diffusion rate constant, which can be obtained from the slope of the inter-article diffusion model, and x_t is a constant related to the quantity of adsorption extent.

4. Results and Discussion

4.1. Characterization of Nanocomposites

To obtain structural information of the composites, XRD patterns of the nanocomposites were taken. The results are depicted in Figure 1. Figure 1A - D indicate the XRD patterns of the pristine ZnO, ZnO/GO, ZnO/GO/zeolite, and GO/zeolite, respectively. As shown in Figure 1A, the appeared sharp peaks are attributed to ZnO NPs (JCPDS Card No. 036-1451). Comparing Figure 1A and B reveals the effect of the presence of GO on the lattice structure of the pristine ZnO NPs, and also the presence and absence of new small peaks may be due to the presence of GO. Figure 1C is related to ZnO/GO/Zeolite. It preserves the characteristic peaks related to pristine ZnO. The remained peaks are attributed to zeolite and GO. Figure 1D is related to GO/zeolite that its peaks were at 2tetah 9.89, 11.22, 13.05, 16.96, 17.36, 20.95, 21.94, 22.45, 22.8, 26.04, 26.64, 30.03, and 32.05, attributed to both of GO and zeolite. In addition, the morphology of the nanocomposites was also studied (Figure 2). As shown in Figure 2A - C, ZnO NPs revealed potato-like particles, which decorated over GO or zeolite in the case of ZnO/GO. ZnO/GO/Zeolite (Figure 2B and C). Finally, Figure 2D showed zeolite NPs that were well dispersed within the GO sheets. In order to obtain surface characteristics and porosity of nanocomposites, N_2- adsorption-desorption on the nanocomposites was studied. The BET and BJH models of the nanocomposites were obtained, and then the active surface area, pore diameters, and pore volume of the adsorbents were calculated (45-47). The results of the study are depicted in Figure 3A and B as well as Table 1. As shown in Figure 3A, a hysteresis loop shape revealed that the samples had mesostructured. In addition, a greater extent of adsorption was achieved with ZnO/nanocomposites compared to the pristine ZnO NPs. This may be due to the creation of the core-shell of ZnO-NPs. with zeolite and GO-NPs, so it can cause ZnO lattice layers to be separated from each other, which in turn causes improved porosity of the nanocomposites. On the other hand, active surface areas for the ZnO/GO are extremely greater than the other nanocomposites. Based on the BJH model, pore volumes of ZnO/GO were extremely greater than pure ZnO NPs (Figure 3B and Table 1). Mean pore diameters of ZnO NPs were increased from 116.5 nm to 140.2 nm, due to the presence of GO. On the other hand, mean pore diameters were decreased in the case of ZnO/GO/zeolite and GO/zeolite, it may be due to the penetration of ZnO NPs and GO NPs into the zeolite tetrahedral frameworks. Hence, the decrease in the mean pores diameter can be justified. Meanwhile, the greater pore volume and surface area of ZnO/GO/zeolite and GO/zeolite, compared to that of ZnO NPs, can be explained by the presence of zeolite and GO sheets, which causes the spread of ZnO NPs over GO sheets to produce an extensive surface. Zeolite could not help ZnO NPs to produce more extensive surfaces than GO, because of penetration of some of ZnO NPs into the zeolite frameworks, as discussed earlier.

4.2. Effect of Adsorbent Dosage

Different amounts of adsorbents were examined to investigate the effect of the adsorbent dosage on the removal of chloroform (Figure 4). As shown in Figure 4, about 0.3 g of the adsorbents was enough to reach the maximum chloroform removal for each of the nano-adsorbents. The figure also shows that ZnO/GO could remove a greater extent of chloroform compared to the other nanocomposites.

4.3. Kinetic Study of Chloroform Removal

Figure 5 shows the fitted data, based on the abovementioned adsorption kinetic models for the different adsorbents. As obvious in the figure, almost all of the adsorbents followed the inter-particle diffusion kinetic model.

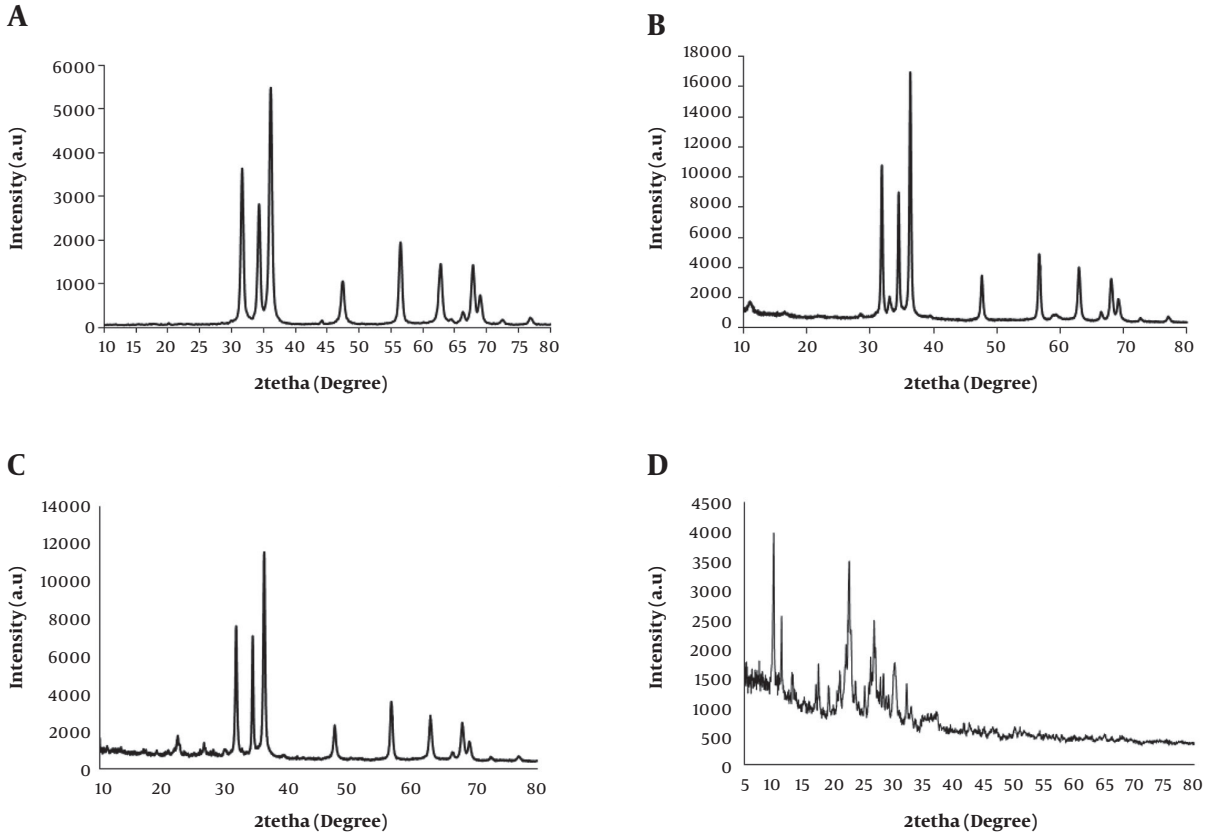

Figure 1. XRD patterns of ZnO NPs (A), ZnO/GO (B), ZnO/GO/zeolite (C), and GO/zeolite (D)

Table 1. Textural Parameters of Samples of The Different Nanocomposites

Sample	Specific Surface Area (a_p) ($m^2 . g^{-1}$)	Mean Pore Diameter (r_p) (nm)	Pore Volume (V_p) ($cm^3 . g^{-1}$)
ZnO/GO	23.34	140.2	0.088
ZnO	8.8	116.5	0.025
ZnO/GO/Zeolite	19.2	80.3	0.046
GO/Zeolite	22.5	87.4	0.047

All of the corresponding kinetic constants of the adsorbents are summarized in Table 2. As shown in the table, ZnO/GO and GO/Zeolite showed a greater adsorption rate constant compared to the other two adsorbents. However, the results of the isotherm study, which are provided in the following sections, confirm the superiority of ZnO/GO to GO/Zeolite, because of the greater maximum capacity of the former compared to the latter.

4.4. Maximum Capacity of the Adsorbents

The maximum capacity of an adsorbent is the maximum amounts (mg) of adsorbate that can be adsorbed on one gram of the material. Different sorbents have various adsorption mechanism or adsorption routes. Different adsorption isotherms are introduced by authors (48-51). In this work, two famous adsorption models, Langmuir (Equation 6) and Freundlich (Equation 7), were studied for the different adsorbents (48, 49). Adsorption models of the adsorbents are shown in Figure 6. As this figure shows, almost all of the nanocomposites follow the Langmuir adsorption model, which predicts a monolayer physical adsorption of the chloroform on the sorbents. This is more rational, because of the hydrophobic character of chloroform, which makes it possible to be adsorbed on the nanocomposites. Different isotherm parameters

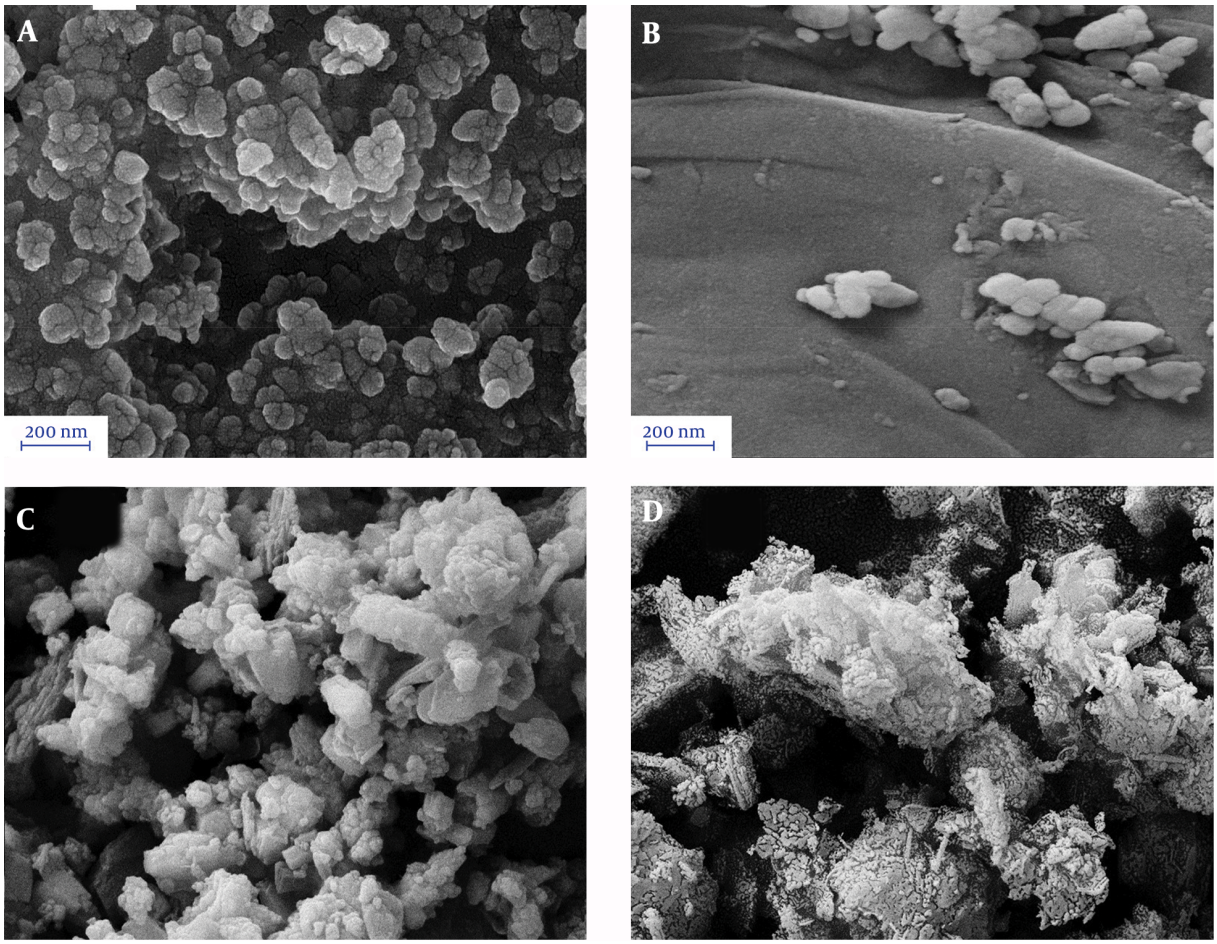

Figure 2. FESEM images of ZnO NPs (A), ZnO/GO (B), and ZnO/GO/zeolite (C), and GO/zeolite (D)

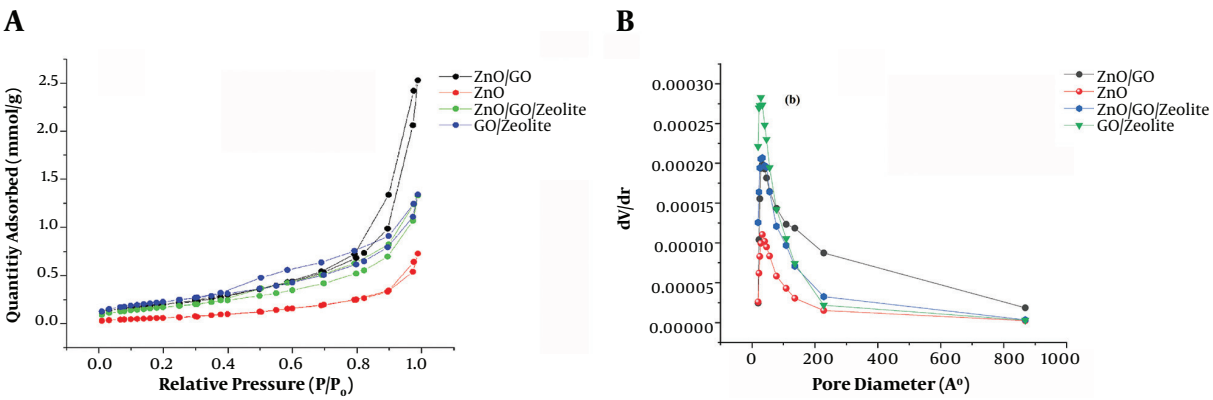

Figure 3. A, BET isotherm based on Nitrogen-adsorptiondesorption on the different adsorbents; B, Pore size distribution of the different nanocomposites

Table 2. Kinetic Parameters of the Different Adsorbents (Nanocomposites)

Adsorbent composition	Pseudo-first order		Pseudo-second order		Interparticle diffusion	
	R_2	K_1	R_2	K_2	R^2	K_p
ZnO	0.859	0.119756	0.835	0.000555	0.996	27.63
ZnO/GO	0.763	0.096726	0.845	0.000281	0.993	35.5
ZnO/GO/Zeolite	0.961	0.156604	0.993	0.006	0.929	27.9
GO/Zeolite	0.894	0.175028	0.928	0.0007	0.996	45.45

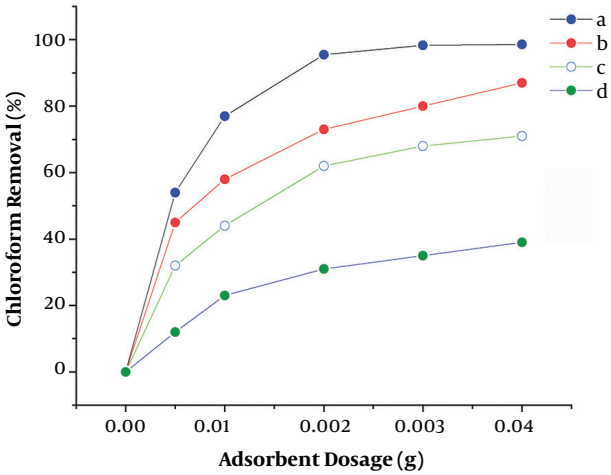

Figure 4. Effect of the different nanocomposite amount on the removal percent of chloroform, (a) ZnO/GO, (b) GO/Zeolite, (c) ZnO/GO/Zeolite, and (d) ZnO NPs

were also computed using the different isotherm models of interest (Table 3). As indicated by the results, ZnO/GO showed a greater adsorption capacity compared to the other nanocomposites. As evident from Table 3, the order of the maximum adsorption capacity of the nanocomposites was predicted as follows: (ZnO/GO) > (ZnO/GO/Zeolite) > (GO/Zeolite) > (ZnO NPs.). These results are consistent with those earlier obtained with BET and BJH models (Table 1).

$$\frac{1}{q_e} = \frac{1}{K_L \ .Q_{max} \ .C_e} + \frac{1}{q_{max}} \quad (6)$$

$$q_e = k_f . C_e^{\frac{1}{n}} \quad (7)$$

4.5. Effect of the pH on the Removal of Chloroform

pH is a crucial condition for all aquatic environments. It also can affect chemical, physical, and microbial properties. For this reason, the pH of water samples was changed from 3 to 10. The different adsorbents showed different trends toward the removal of chloroform in a different pH. As indicated in the inset of Figure 7, about all of the adsorbents had better adsorption of chloroform in the pH range between 7 to 8 compared to the other pHs. This is due to the solubility of ZnO in acidic and alkaline media. ZnO/GO and GO/Zeolite even had shown remarkable adsorption in acidic regions because of the presence of GO in these harsh conditions. On the other hand, in alkaline regions, the removal of chloroform was diminished remarkably for all adsorbents. This may be due to the negative charge of the nanocomposites resulted from the adsorption of hydroxide ions in high concentrations in these regions. Hence optimal pH range for the best removal percentage for all of the adsorbents was concluded to be 7 to 8.

4.6. Regenerability of the Nanocomposites

From a commercial viewpoint, using regenerable adsorbents is necessary to reduce the cost of water treatment. Hence, the regeneration of the adsorbents is highly important. For this reason, four removal cycles were performed using sixteen industrial wastewater samples that were spiked with 50 $mg.dm^{-3}$ of chloroform. Afterward, four aliquots of 50 mL of the wastewater samples, containing chloroform, were treated with the different adsorbents in each removal cycle. After each chloroform-removal cycle, the nano adsorbents were regenerated by incubating in an electric oven at 150°C for 1 hour, during which the adsorbents were degassed. Then, the removal tests were performed with the rest of the wastewater samples in the same way. The results of the study are depicted in the inset of Figure 7. As shown in the figure, the approximately adsorptive character of the nano adsorbents remained intact after their repetitive usages. Indeed, the porosity of the nano adsorbents did not change during several usages, which confirms their stability and applicability.

4.7. Comparing ZnO/GO Nanocomposites with other Adsorbents

Different characteristics of the ZnO/GO nanocomposite were compared with reported adsorbents used for the removal of chloroform, and the results are summarized in Table 4 (23, 50-52). As seen, the proposed ZnO/GO had a

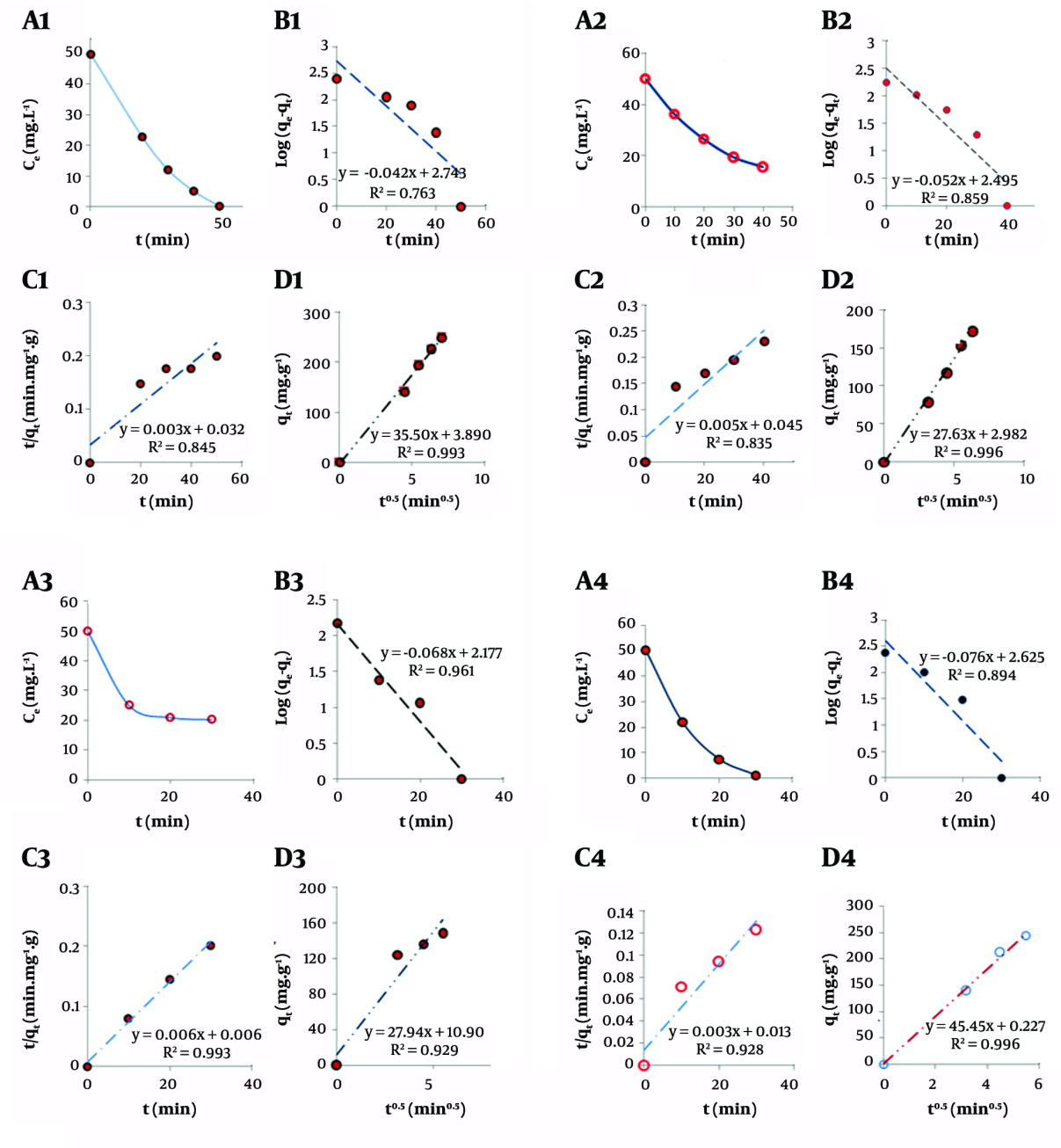

Figure 5. Kinetic models for the adsorption of chloroform on ZnO/GO, (a1-a4) concentration-time profile of chloroform removal, (b1-b4) pseudo-first-order model, (c1-c4) pseudo-second-order model, and (d1-d4) inter-particle diffusion model for ZnO/GO, ZnO, ZnO/GO/Zeolite, and GO/Zeolite, respectively

greater maximum adsorption capacity and surface characteristics compared to the other adsorbents. The ZnO/GO showed a greater chloroform removal efficiency than the reported adsorbents. These results can be explained by the fact that both GO and ZnO have adsorption capacity toward chloroform, and GO acts as good support for dispersing ZnO NPs. Hence, the prepared nanocomposite indicated better surface characteristics and removal efficiency compared to the other adsorbents.

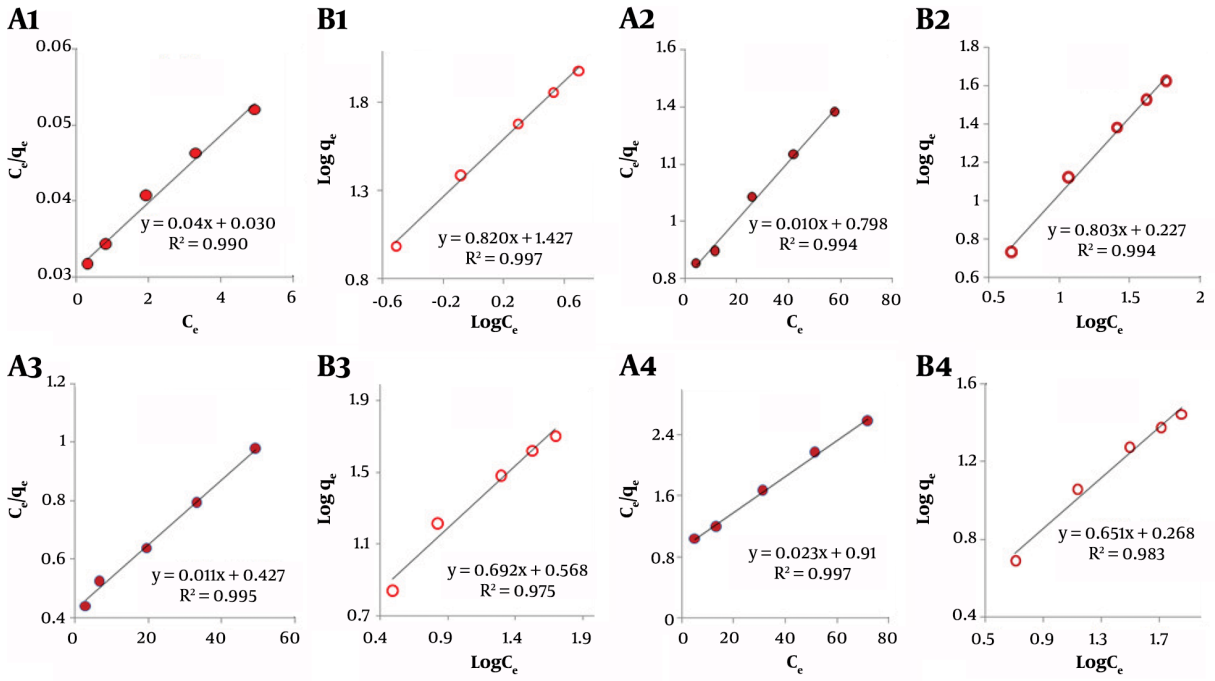

Figure 6. Different isotherm models, (a1-a4) Langmuir models, and (b1-b4) Freundlich models for ZnO/GO, ZnO NPs, ZnO/GO/Zeolite, and GO/Zeolite, respectively

Table 3. Isotherm Parameters of the Different Adsorbents for the Removal of Chloroform

Adsorbent composition	Langmuir			Freundlich		
	q_{max}	K_L	R^2	1/n	K_F	R^2
ZnO	43.47	0.025	0.997	0.651	1.853	0.983
ZnO/GO	250	0.1333	0.993	0.82	26.73	0.997
ZnO/GO/Zeolite	100	0.0125	0.994	0.803	1.686	0.994
GO/Zeolite	90.9	0.0257	0.995	0.692	3.698	0.975

Table 4. Comparison of Zno/GO Characteristics with the Reported Adsorbents Used for Chloroform Removal

Adsorbent	q_{max} (mg. g^{-1})	Specific Surface Area (m^2. g^{-1})	Mean Pore Diameter (nm)	Pore Volume (cm^3)	Chloroform Removal (%)	Ref.
Snow	3.77×10^{-3}	-	-	-	-	(23)
Asf	2.33	0.81	-	-	-	(50)
Asf/Nitro	9.16	3.11			-	(50)
Silica loaded AC	8.66	-	-	-	95	(51)
AC	-	62.348	61.53	95	50	(51, 52)
AC/ZnO	86.28	15.178	80.16	0.3	80.7	(52)
ZnO/GO	250	23.34	140.2	0.088	98	This work

Abbriviations: Asf, Asphaltene; AC, Activated carbon.

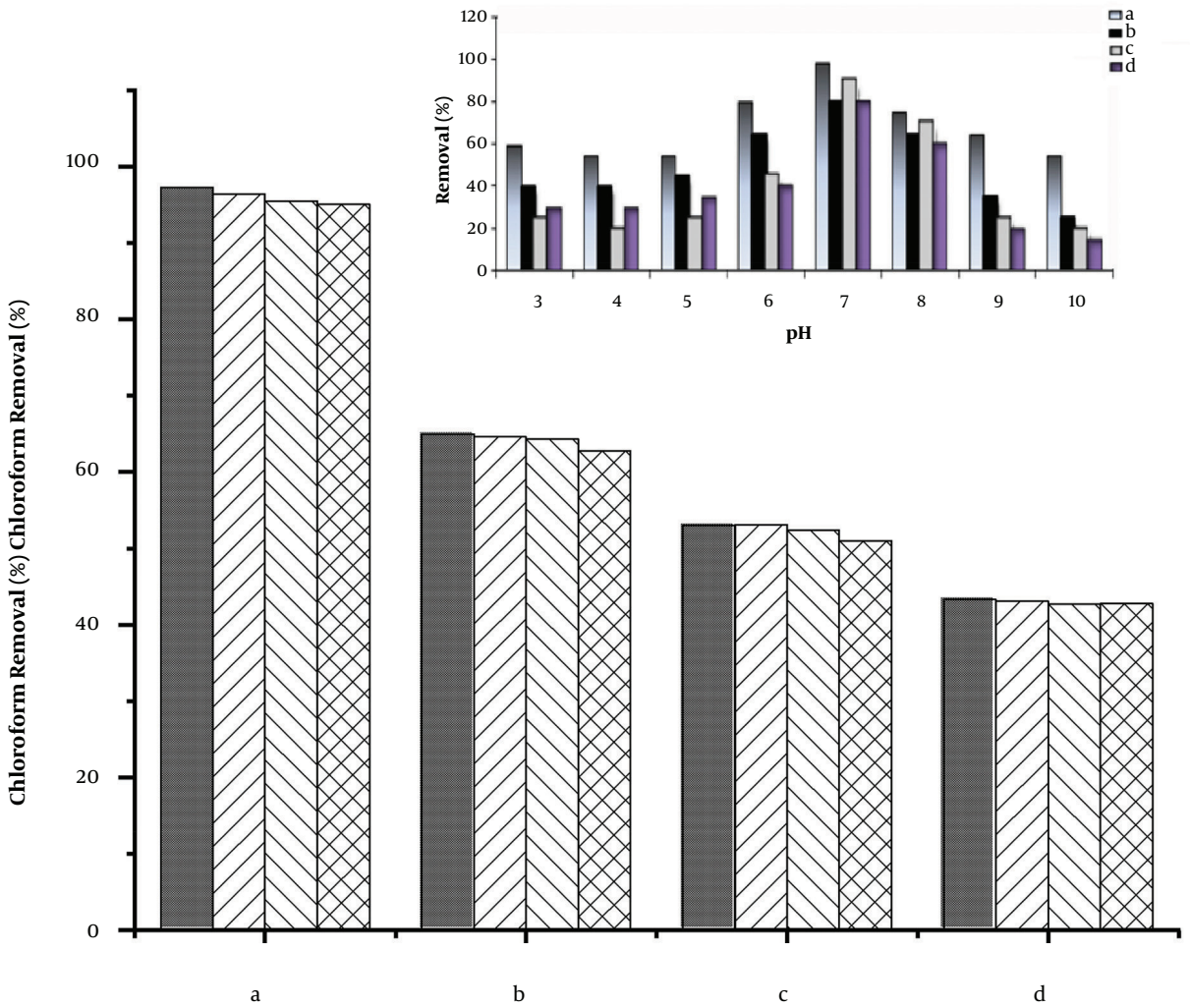

Figure 7. Regenerability of the nano adsorbents for removal of chloroform from 50 mg.dm-3 chloroform solutions after four times use (a) ZnO/GO, (b) ZnO/GO/Zeolite, (c) GO/Zeolite,(d) Zn NPs, Inset: Effect of pH on the removal of chloroform by using the different adsorbents: (a) ZnO/GO, (b) GO/Zeolite, (c) ZnO NPs and (d) ZnO/GO/Zeolite

5. Conclusion

Different nanocomposites of ZnO-inorganic sorbents were synthesized and used for the removal of chloroform. N2-adsorption-desorption isotherms of the nanocomposites were used to essay and compare their textural properties. The results revealed that all of the synthesized nanocomposites are mesoporous. Active surface area, pore size, and pore volumes of the nanocomposites were determined using BET and BJH models. Kinetic and isotherm models of the nanocomposites also were investigated. ZnO/GO showed the best performance to remove chloroform from water samples due to its superior porosity.

Acknowledgments

The authors acknowledge Islamic Azad University, Shoushtar branch for partial support of the work.

Footnotes

Authors' Contribution: Ramin Yousefi, Methodology; Abbas Shirmardi, and Majid Razaz; Formal analysis and investigation: Frazad Salehi-Babarsad, Ehsan Derikvand; Writing - original draft preparation: Abbas Shirmardi, Ehsan Derikvand, and Ramin Yousefi; Writing - review and editing: Ramin Yousefi, Abbas Shirmardi, and Majid Razaz;

Resources: Farzad Salehi-Babarsad; Supervision: Ehsan Derikvand, Majid Razaz, Ramin Yousefi, Abbas Shirmardi.

Conflict of Interests: The authors declare no conflict of interest.

Funding/Support: This study was not funded by any organization.

References

1. Zhao W, Chen I, Huang F. Toward large-scale water treatment using nanomaterials. *Nano Today*. 2019;**27**:11–27. doi: 10.1016/j.nantod.2019.05.003.
2. Khan MAQ, Khan SF, Shattari F. *Halogenated Hydrocarbons*. Encyclopaedia of Ecology, Elsevier; 2008. p. 1831–43. doi: 10.1016/b978-008045405-4.00399-2.
3. Alhooshani KR. Adsorption of chlorinated organic compounds from water with cerium oxide-activated carbon composite. *Arab J Chem*. 2019;**12**(8):2585–96. doi: 10.1016/j.arabjc.2015.04.013.
4. Pires J, Carvalho A, de Carvalho MB. Adsorption of volatile organic compounds in Y zeolites and pillared clays. *Microporous Mesoporous Mater*. 2001;**43**(3):277–87. doi: 10.1016/s1387-1811(01)00207-4.
5. Sonoyama N, Ezaki K, Sakata T. Continuous electrochemical decomposition of dichloromethane in aqueous solution using various column electrodes. *Adv Environ Res*. 2001;**6**(1):1–8. doi: 10.1016/s1093-0191(00)00065-4.
6. Rexwinkel G, Heesink BB, van Swaaij WP. Adsorption of halogenated hydrocarbons from aqueous solutions by wetted and nonwetted hydrophobic and hydrophilic sorbents: Equilibria. *J Chem Eng Data*. 1999;**44**(6):1139–45. doi: 10.1021/je9900373.
7. Babcock DB, Singer PC. Chlorination and coagulation of humic and fulvic acids. *J Am Water Works Ass*. 1979;**71**(3):149–52. doi: 10.1002/j.1551-8833.1979.tb04318.x.
8. Mackenzie K, Frenzel H, Kopinke F. Hydrodehalogenation of halogenated hydrocarbons in water with Pd catalysts: Reaction rates and surface competition. *Appl Catal B*. 2006;**63**(3-4):161–7. doi: 10.1016/j.apcatb.2005.10.004.
9. Salehi-Babarsad F, Derikvand E, Razaz M, Yousefi R, Shirmardi A. Heavy metal removal by using ZnO/organic and ZnO/inorganic nanocomposite heterostructures. *Int J Environ Anal Chem*. 2019;**100**(6):702–19. doi: 10.1080/03067319.2019.1639685.
10. Nagpal M, Kakkar R. Use of metal oxides for the adsorptive removal of toxic organic pollutants. *Sep Purif Technol*. 2019;**211**:522–39. doi: 10.1016/j.seppur.2018.10.016.
11. Baghel A, Singh B, Pandey P, Dhaked RK, Gupta AK, Ganeshan K, et al. Adsorptive removal of water poisons from contaminated water by adsorbents. *J Hazard Mater*. 2006;**137**(1):396–400. doi: 10.1016/j.jhazmat.2006.02.070. [PubMed: 16675110].
12. Sophia AC, Lima EC. Removal of emerging contaminants from the environment by adsorption. *Ecotoxicol Environ Saf*. 2018;**150**:1–17. doi: 10.1016/j.ecoenv.2017.12.026. [PubMed: 29253687].
13. Tian YL, Ren JF, Yue WW, Chen MN, Hu GC, Yuan XB. Adsorption of chloroform on N-doped and Al-doped graphene: A first-principle study. *Chem Phys. Lett*. 2017;**685**:344–8. doi: 10.1016/j.cplett.2017.08.001.
14. Jose J, Ramanujam S, Philip L. Applicability of pulsed corona discharge treatment for the degradation of chloroform. *Chem Eng J*. 2019;**360**:1341–54. doi: 10.1016/j.cej.2018.10.199.
15. Lee H, In J, Lee S, Kim J, Lee C. An anti-corrosive reactor for the decomposition of halogenated hydrocarbons with supercritical water oxidation. *J Supercrit Fluid*. 2005;**36**(1):59–69. doi: 10.1016/j.supflu.2005.04.001.
16. Adachi A, Takagi S, Okano T. Adsorption and adsorption mechanism of rice bran for chloroform from tap water. *Chemosphere*. 2002;**46**(1):87–92. doi: 10.1016/s0045-6535(01)00080-7.
17. Buekens A, Huang H. Comparative evaluation of techniques for controlling the formation and emission of chlorinated dioxins/furans in municipal waste incineration. *J Hazard Mater*. 1998;**62**(1):1–33. doi: 10.1016/s0304-3894(98)00153-8.
18. Crini G, Lichtfouse E, Wilson LD, Morin-Crini N. Adsorption-oriented processes using conventional and non-conventional adsorbents for wastewater treatment. *Environ Chem Sustain*. 2018;**18**:23–71. doi: 10.1007/978-3-319-92111-2_2.
19. Devi P, Saroha AK. Utilization of sludge based adsorbents for the removal of various pollutants: A review. *Sci Total Environ*. 2017;**578**:16–33. doi: 10.1016/j.scitotenv.2016.10.220. [PubMed: 27838056].
20. Lemus J, Martin-Martinez M, Palomar J, Gomez-Sainero L, Gilarranz MA, Rodriguez JJ. Removal of chlorinated organic volatile compounds by gas phase adsorption with activated carbon. *Chem Engin J*. 2012;**211-212**:246–54. doi: 10.1016/j.cej.2012.09.021.
21. Zielhuis SW, Nijsen JF, Dorland L, Krijger GC, van Het Schip AD, Hennink WE. Removal of chloroform from biodegradable therapeutic microspheres by radiolysis. *Int J Pharm*. 2006;**315**(1-2):67–74. doi: 10.1016/j.ijpharm.2006.02.010. [PubMed: 16549282].
22. Rodríguez-Chueca J, Mediano A, Pueyo N, García-Suescun I, Mosteo R, Ormad MP. Degradation of chloroform by Fenton-like treatment induced by electromagnetic fields: A case of study. *Chem Engin Sci*. 2016;**156**:89–96. doi: 10.1016/j.ces.2016.09.016.
23. Wang N, Liu H, Kang C, Wang Y, Kunkun X, Tian T. Removal of γ-HCH, 1,4-Dichlorobenzene and trichloromethane from air via the adsorption of snow. *Atmos Environ*. 2019;**213**:377–83. doi: 10.1016/j.atmosenv.2019.06.012.
24. Li J, Wu F, Mailhot G, Deng N. Photodegradation of chloroform in aqueous solution: impact of montmorillonite KSF particles. *J Hazard Mater*. 2010;**174**(1-3):368–74. doi: 10.1016/j.jhazmat.2009.09.061. [PubMed: 19828241].
25. Jefferson B, Jarvis P, Bhagianathan GK, Smith H, Autin O, Goslan EH, et al. Effect of elevated UV dose and alkalinity on metaldehyde removal and THM formation with UV/TiO2 and UV/H2O2. *Chem Engin J*. 2016;**288**:359–67. doi: 10.1016/j.cej.2015.11.071.
26. Jafari S, Derakhshankhah H, Alaei L, Fattahi A, Varnamkhasti BS, Saboury AA. Mesoporous silica nanoparticles for therapeutic/diagnostic applications. *Biomed Pharmacother*. 2019;**109**:1100–11. doi: 10.1016/j.biopha.2018.10.167. [PubMed: 30551360].
27. Morsi RE, Mohamed RS. Nanostructured mesoporous silica: influence of the preparation conditions on the physical-surface properties for efficient organic dye uptake. *R Soc Open Sci*. 2018;**5**(3):172021. doi: 10.1098/rsos.172021. [PubMed: 29657800]. [PubMed Central: PMC5882724].
28. Biener J, Wittstock A, Baumann T, Weissmüller J, Bäumer M, Hamza A. Surface Chemistry in Nanoscale Materials. *Materials*. 2009;**2**(4):2404–28. doi: 10.3390/ma2042404.
29. Sridar R, Ramanane U, Rajasimman M. ZnO nanoparticles – Synthesis, characterization and its application for phenol removal from synthetic and pharmaceutical industry wastewater. *Environ Nanotechnol Monit Manag*. 2018;**10**:388–93. doi: 10.1016/j.enmm.2018.09.003.
30. Basheer AA. New generation nano-adsorbents for the removal of emerging contaminants in water. *J Mol Liq*. 2018;**261**:583–93. doi: 10.1016/j.molliq.2018.04.021.
31. Wang H, Yuan X, Wu Y, Huang H, Zeng G, Liu Y, et al. Adsorption characteristics and behaviors of graphene oxide for Zn(II) removal from aqueous solution. *Appl Surf Sci*. 2013;**279**:432–40. doi: 10.1016/j.apsusc.2013.04.133.
32. Musevi SJ, Mohammad-Rezaei R, Razmi H. Magnetic solid-phase extraction of malachite green using soluble eggshell membrane protein doped with magnetic graphene oxide nanocomposite. *Int J Environ Anal Chem*. 2018;**98**(13):1242–52. doi: 10.1080/03067319.2018.1543420.
33. Dubey S, Banerjee S, Upadhyay SN, Sharma YC. Application of common nano-materials for removal of selected metallic species from wa-

ter and wastewaters: A critical review. *J Mol Liq*. 2017;**240**:656–77. doi: 10.1016/j.molliq.2017.05.107.
34. Hamid H, Çelik-Butler Z. Characterization and performance analysis of Li-doped ZnO nanowire as a nano-sensor and nano-energy harvesting element. *Nano Energy*. 2018;**50**:159–68. doi: 10.1016/j.nanoen.2018.05.023.
35. Huang Y, Zeng X, Guo L, Lan J, Zhang L, Cao D. Heavy metal ion removal of wastewater by zeolite-imidazolate frameworks. *Sep Purif Technol*. 2018;**194**:462–9. doi: 10.1016/j.seppur.2017.11.068.
36. Kobielska PA, Howarth AJ, Farha OK, Nayak S. Metal–organic frameworks for heavy metal removal from water. *Coord Chem Rev*. 2018;**358**:92–107. doi: 10.1016/j.ccr.2017.12.010.
37. Saad AHA, Azzam AM, El-Wakeel ST, Mostafa BB, Abd El-latif MB. Removal of toxic metal ions from wastewater using ZnO@Chitosan core-shell nanocomposite. *Environ Nanotechnol Monit Manag*. 2018;**9**:67–75. doi: 10.1016/j.enmm.2017.12.004.
38. Molaei P, Cheraghizade M, Yousefi R. Impact of rGO on photocatalytic performance of Cd-doped ZnO nanostructures synthesized via a simple aqueous co-precipitation route. *Mater Res Express*. 2018;**6**(2):25051. doi: 10.1088/2053-1591/aaf1d9.
39. Brunauer S, Deming LS, Deming W, Teller E. On a theory of the van der waals adsorption of gases. *J Am Chem Soc*. 1940;**62**(7):1723–32. doi: 10.1021/ja01864a025.
40. Ho YS, McKay G, Wase DAJ, Forster CF. Study of the sorption of divalent metal ions on to peat. *Adsorp Sci Technol*. 2016;**18**(7):639–50. doi: 10.1260/0263617001493693.
41. Onal Y. Kinetics of adsorption of dyes from aqueous solution using activated carbon prepared from waste apricot. *J Hazard Mater*. 2006;**137**(3):1719–28. doi: 10.1016/j.jhazmat.2006.05.036. [PubMed: 16806677].
42. Yao C. Extended and improved Langmuir equation for correlating adsorption equilibrium data. *Sep Purif Technol*. 2000;**19**(3):237–42. doi: 10.1016/s1383-5866(00)00060-5.
43. Shafqat MN, Pierzynski GM. The Freundlich adsorption isotherm constants and prediction of phosphorus bioavailability as affected by different phosphorus sources in two Kansas soils. *Chemosphere*. 2014;**99**:72–80. doi: 10.1016/j.chemosphere.2013.10.009. [PubMed: 24238913].
44. Naderi M. Surface area: Brunauer-emmett-teller (BET). In: Tarleton S, editor. *Progress in filtration and separation*. UK: Academic Press; 2015. p. 585–608. doi: 10.1016/b978-0-12-384746-1.00014-8.
45. Groen JC, Peffer LA, Pérez-Ramı´rez J. Pore size determination in modified micro- and mesoporous materials. Pitfalls and limitations in gas adsorption data analysis. *Microporous Mesoporous Mater*. 2003;**60**(1-3):1–17. doi: 10.1016/s1387-1811(03)00339-1.
46. Sari A, Tuzen M. Biosorption of cadmium(II) from aqueous solution by red algae (Ceramium virgatum): equilibrium, kinetic and thermodynamic studies. *J Hazard Mater*. 2008;**157**(2-3):448–54. doi: 10.1016/j.jhazmat.2008.01.008. [PubMed: 18280037].
47. Lagergren S. About the theory of so-called adsorption of solution substances. *Sven Vetenskapsakad Handingarl*. 1898;**24**:1–39.
48. Sips R. On the structure of a catalyst surface. *J Chem Phys*. 1948;**16**(5):490–5. doi: 10.1063/1.1746922.
49. Dubinin MM. The potential theory of adsorption of gases and vapors for adsorbents with energetically nonuniform surfaces. *Chem Rev*. 1960;**60**(2):235–41. doi: 10.1021/cr60204a006.
50. Plata-Gryl M, Momotko M, Makowiec S, Boczkaj G. Highly effective asphaltene-derived adsorbents for gas phase removal of volatile organic compounds. *Sep Purif Technol*. 2019;**224**:315–21. doi: 10.1016/j.seppur.2019.05.041.
51. Abdelbassit MS, Alhooshani KR, Saleh TA. Silica nanoparticles loaded on activated carbon for simultaneous removal of dichloromethane, trichloromethane, and carbon tetrachloride. *Adv Powder Technol*. 2016;**27**(4):1719–29. doi: 10.1016/j.apt.2016.06.003.
52. Saleh TA, Alhooshani KR, Abdelbassit MS. Evaluation of AC/ZnO composite for sorption of dichloromethane, trichloromethane and carbon tetrachloride: kinetics and isotherms. *J Taiwan Inst Chem Eng*. 2015;**55**:159–69. doi: 10.1016/j.jtice.2015.04.004.